

STUDY OF IONIZATION COOLING WITH THE MICE EXPERIMENT

C. T. Rogers*, Rutherford Appleton Laboratory, Didcot, UK
on behalf of the MICE Collaboration

Abstract

The international Muon Ionization Cooling Experiment (MICE) will demonstrate the ionization cooling of muons; the only known technique that can provide high brightness muon beams suitable for applications such as a Neutrino Factory or Muon Collider. MICE is underway at the Rutherford Appleton Laboratory and has recently taken the data necessary to characterise the physical processes that underlie the ionization-cooling effect. Measurements of the change in normalised transverse amplitude are presented in two configurations. The measurements of the ionization-cooling effect are discussed.

MUON IONIZATION COOLING

Ionization cooling [1] is the only known technique that can cool a muon beam on a timescale competitive with the muon lifetime [2–5]. Muon cooling has never been demonstrated previously. In ionization cooling, a beam is passed through an absorber causing energy to be lost due to ionization of atomic electrons. This yields a reduction in normalized transverse emittance. Multiple Coulomb scattering from atoms causes an increase in angular divergence of the beam, and hence emittance growth. The change in normalized RMS emittance ε_{\perp} in distance dz is [1]

$$\frac{d\varepsilon_{\perp}}{dz} \approx -\frac{\varepsilon_{\perp}}{\beta^2 E_{\mu}} \left\langle \frac{dE}{dz} \right\rangle + \frac{\beta_{\perp} (13.6 \text{ MeV}/c)^2}{2\beta^3 E_{\mu} m_{\mu} X_0} \quad (1)$$

where β_{\perp} is the transverse optical Twiss function, βc , E_{μ} , m_{μ} are the particle velocity, energy and mass, and X_0 is the radiation length. There exists an equilibrium RMS emittance ε_{eqm}

$$\varepsilon_{eqm} \approx \frac{1}{2} \frac{13.6^2}{m_{\mu} X_0} \frac{\beta_{\perp}}{\beta \langle dE/dz \rangle} \quad (2)$$

at which $d\varepsilon_{\perp}/dz = 0$. If a beam with emittance below equilibrium is incident on an absorber, its emittance increases on passage through the absorber. Otherwise the emittance decreases.

EXPERIMENTAL APPARATUS

MICE Step IV [6, 7] consists of a transfer line to bring particles from the ISIS synchrotron at Rutherford Appleton Laboratory to the experiment. A schematic of the apparatus is shown in Fig. 1. The equipment to reduce beam emittance consists of a section of a solenoid focussing ionization cooling cell. Detectors, placed upstream and downstream of the emittance reduction apparatus, measure the momentum, position and species of particles entering and leaving the cooling channel, enabling the measurement of change in normalized beam emittance of the ensemble.

* chris.rogers@stfc.ac.uk

Transfer Line

Pions are created by dipping a titanium target into the ISIS proton synchrotron. A dedicated transfer line has been constructed to transport the resultant particles to the cooling apparatus [8–10]. The incoming particle momentum can be selected by varying the field in a pair of dipoles. Higher magnetic field selects higher particle momentum. A series of tungsten and brass irises are positioned in the transfer line, enabling the selection of different emittances for the ensemble.

Up to around 100 particles are observed per second. MICE accumulates data in runs, each run consisting of a single experimental configuration and lasting of order hours. Several runs are taken for each solenoid configuration. MICE has taken data over thousands of runs, with many different configurations. The number of triggers recorded by MICE in 2015 and 2016 is shown in Fig. 2.

Cooling Channel

The cooling channel consists of three superconducting solenoid modules [11, 12]. Two spectrometer solenoid modules each generate a region of uniform 3 T field in which diagnostic trackers are situated and a matching region that transports the beam from the solenoid to the focus coil module. The focus coil module, positioned between the solenoids, provides additional focussing to increase the angular divergence of the beam at the absorber, improving the amount of emittance reduction that can be achieved. The magnetic field model is shown in Fig. 3.

The absorber was a single 65 mm thickness lithium hydride disk. Lithium hydride was chosen as an absorber material as it provides less multiple Coulomb scattering for a given energy loss, due to the smaller electric charge of the nucleus.

Diagnostic Apparatus

Upstream of the cooling apparatus, two time-of-flight detectors (TOFs) [13, 14] enable the measurement of particle velocity, which is validated by a threshold Cerenkov counter [15]. Scintillating fibre trackers, positioned either side of the absorber module, enable the measurement of particle position and momentum upstream and downstream of the absorber. Further downstream an additional TOF detector, a KLOE Light pre-shower detector and Electron Muon Ranger enable rejection of electron impurities.

The trackers consist of 5 stations [16, 17]. Each station consists of 3 views, each view rotated by 120° with respect to the previous view. Each view consists of 2 layers of scintillating fibres. Gangs of 7 scintillating fibres are read out together by cryogenically operated Visible Light Photon Counters, enabling the position of incident particles to be measured

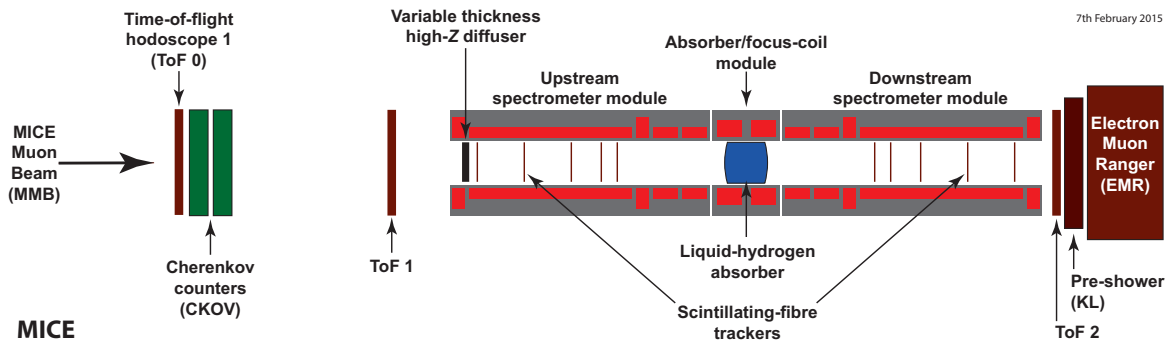


Figure 1: The MICE apparatus.

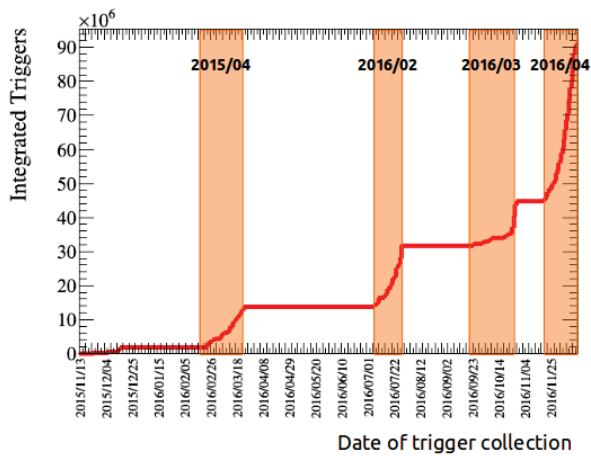


Figure 2: The integrated number of triggers taken by MICE since 2015. Text in the figure identifies the ISIS user-cycle.

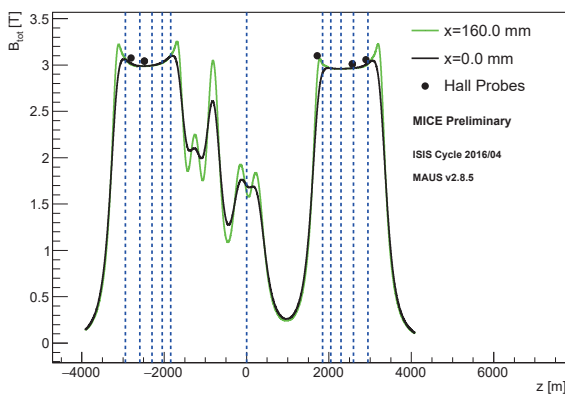


Figure 3: Modelled magnetic field for the configuration on the axis and with 160 mm horizontal displacement from the axis. Hall probes, situated 160 mm from the beam axis, show a 2 % discrepancy with the model. Dashed lines show position of the tracker stations and absorber.

with a resolution of 0.3 to 0.4 mm. The trackers are situated in uniform 3 T fields such that particles make a helical path. The magnitude of the field is measured using Hall probes situated in the region of the tracker. By measuring the radius

and pitch of the helix, the momentum of the particle can be deduced. The trackers have sufficient redundancy to enable the track reconstruction to be internally validated in order to estimate the efficacy of the reconstruction. The uncertainty on the momentum of each track is around 1-2 MeV/c.

Each TOF consists of two planes. Each TOF plane is made up of a number of scintillator slabs. Photomultiplier tubes at either end of the TOF slabs produce a signal when particles pass through the TOF. The time at which muons pass through the apparatus can be measured with a resolution of 60 ps.

Operation of the Equipment

In this paper the evolution of phase space density is reported for a single configuration of the cooling apparatus. The transfer line settings were varied to mimic different beam conditions. Results from two transfer line configurations are reported, with the accumulated muon sample having nominal emittances of 3 mm and 6 mm at momenta around 140 MeV/c in the upstream spectrometer solenoid. These configurations are denoted ‘3-140’ and ‘6-140’ respectively.

RESULTS

Particle Ensemble Selection

As MICE measures each particle event individually, it is possible to select a particle ensemble from the collection of measured tracks. This enables the study of momentum spread and transverse beam parameters on the cooling. In this analysis, muons have been selected with:

- momentum in the range 135 to 145 MeV/c;
- time-of-flight between TOF0 and TOF1 consistent with muons in this momentum range; and
- a single, good quality track formed in the upstream diagnostics.

Optics

The design optics for the magnet currents described above is shown in Fig. 4. After the diffuser, particles are transported through the upstream tracker region and two matching coils

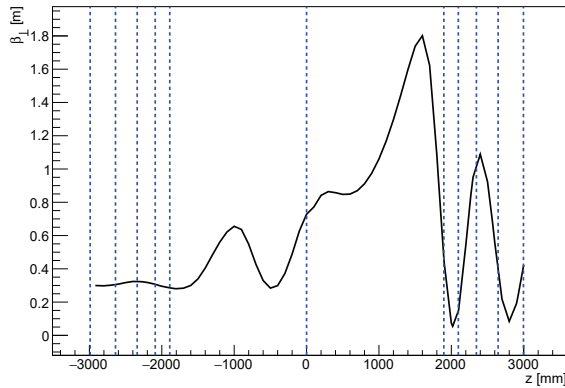


Figure 4: Design optics for the configuration. Dashed lines show position of the tracker stations and absorber.

which bring the particles to a focus just upstream of the lithium hydride absorber. The equilibrium emittance is reduced by keeping the particles well-focussed in the region of the absorber. The design optics yields β_{\perp} of 0.73 m at the absorber. The particles are transported through to the downstream diagnostics where they are measured. Oscillations in β_{\perp} occur downstream of the absorber as the downstream matching coils were not powered for this run period, causing some transmission losses.

Amplitude Evolution

In order to demonstrate emittance reduction, MICE has measured the distribution of amplitude upstream and downstream of the absorber. The 4D amplitude of a particle with phase space vector $\vec{u} = (x, p_x, y, p_y)$ is given by

$$A_{\perp} = \epsilon_{\perp} \vec{u}^T \mathbf{V}^{-1} \vec{u} \quad (3)$$

where \mathbf{V} is the 4D covariance matrix. In order to prevent the tails of the distribution from skewing the core, only those events with amplitude less than A_{\perp} have been included in the calculation of \mathbf{V}^{-1} for a given event. While reduction in RMS emittance can be caused by scraping, increase in the number of muons with low amplitude unambiguously demonstrates increase in muon density and cooling.

The amplitude distribution measured upstream and downstream of the absorber is shown in Fig. 5 for two different configurations, with an initial normalised transverse emittance of 3 mm and 6 mm and an initial momentum of 140 MeV/c. The equilibrium emittance calculated by eq. (2) for the optics presented in Fig. 4 is ~ 6 mm. For the 3-140 setting, muons with low amplitude upstream of the absorber are observed to move to higher amplitude when measured downstream, as the sample emittance is below equilibrium. Muons sampled from the (6-140) setting are seen to stay with roughly the same amplitude, as the sample is near the equilibrium emittance. There is some dilution due to scraping at high amplitude.

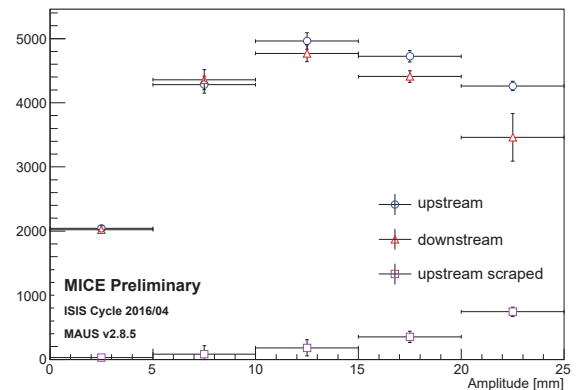
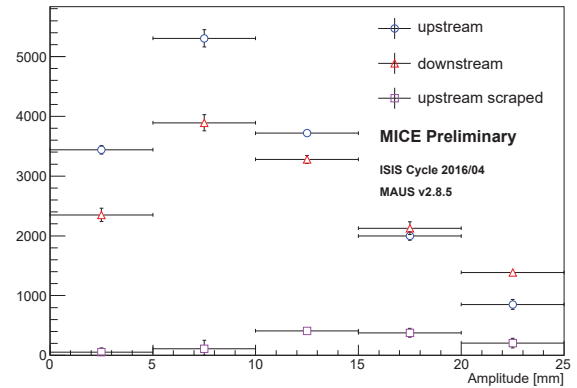


Figure 5: Change in amplitude distribution for the ‘3-140’ configuration (top) and for the ‘6-140’ configuration (bottom). The transmission is around 90 % and 80 % respectively. (Blue circles) amplitude of all upstream events; (red triangles) amplitude of all downstream events; (magenta squares) amplitude of upstream events that are not observed downstream.

CONCLUSIONS

The MICE experiment has measured the change in amplitude distributions of the MICE muon beam across an absorber, showing beam dilution below equilibrium emittance and emittance conservation around equilibrium emittance. The results are qualitatively consistent with expectations. The collaboration continues to reduce the systematic uncertainties associated with the data following more detailed analysis.

Data taking will continue through 2017 with liquid hydrogen absorbers in a number of configurations. A pair of RF cavities have been constructed. The collaboration seeks to upgrade the existing equipment to demonstrate energy recovery along with emittance reduction.

REFERENCES

- [1] D. Neuffer, “Principles and Applications of Muon Cooling,” Part. Accel. 14 (1983) 75–90.

- [2] S. Geer, “Neutrino beams from muon storage rings: Characteristics and physics potential,” *Phys. Rev. D* 57 (1998) 6989–6997, arXiv:hep-ph/9712290.
- [3] M. Apollonio et al., “Oscillation physics with a neutrino factory,” arXiv:hep-ph/0210192.
- [4] D. V. Neuffer and R. B. Palmer, “A High-Energy High-Luminosity $\mu^+ \mu^-$ Collider,” in 4th European Particle Accelerator Conference (EPAC 94) London, England, June 27-July 1, 1994, vol. C940627, pp. 52–54. 1995.
- [5] R. B. Palmer, “Muon Colliders,” *Rev. Accel. Sci. Tech.* 7 (2014) 137–159.
- [6] MICE Collaboration, “MICE: An International Muon Ionization Cooling Experiment” <http://mice.iit.edu/micenotes/public/pdf/MICE0021/MICE0021.pdf>, 2003. MICE Note 21.
- [7] D. Rajaram and V. C. Palladino, “The Status of MICE Step IV,” in Proceedings, 6th International Particle Accelerator Conference (IPAC 2015): Richmond, Virginia, USA, May 3-8, 2015, pp. 4000–4002. 2015.
- [8] M Bogomilov et al., “The MICE Muon Beam on ISIS and the beam-line instrumentation of the Muon Ionization Cooling Experiment”, *Journal of Instrumentation*, Volume 7, Number 5, P05009, 2012.
- [9] D. Adams et al., “Characterisation of the muon beams for the Muon Ionization Cooling Experiment”, *European Journal of Physics C*, Volume 73, Number 10, pp. 2582, 2013.
- [10] M. Bogomilov et al., “Pion contamination in the MICE muon beam”, *Journal of Instrumentation* Volume 11, P03001, 2016.
- [11] S. Virostek, S. Prestemon and R. Preece, “Assembly and Test of a Modified Spectrometer Solenoid for MICE”, *Proceedings of IPAC2013*, pp.3621-3623, 2013.
- [12] V. Bayliss et al., “MICE Absorber and Focus Coil As Built Configuration”, *MICE Note* 463, 2015.
- [13] R. Bertoni et al., “The design and commissioning of the MICE upstream time-of-flight system,” *Nucl. Instrum. Meth.* A615 (2010) 14–26, arXiv:1001.4426.
- [14] R. Bertoni, M. Bonesini, A. de Bari, G. Cecchet, Y. Karadzhov, and R. Mazza, “The construction of the MICE TOF2 detector.”, <http://mice.iit.edu/micenotes/public/pdf/MICE0286/MICE0286.pdf>, 2010.
- [15] L. Cremaldi et al., *IEEE Trans. Nucl. Sci.* 56 (2009) 1475
- [16] M. Ellis et al., “The design, construction and performance of the MICE scintillating fibre trackers,” *Nucl. Instrum. Meth.* A659 (2011) 136–153, arXiv:1005.3491.
- [17] A. Dobbs et al., The reconstruction software for the MICE scintillating fibre trackers, *Journal of Instrumentation* Volume 11 T12001.